Multifractal analysis of ZnO thin films doped with Mg deposited by sol-gel spin coating on a glass substrate

Ştefan Ţălu
Technical University of Cluj-Napoca: Universitatea Tehnica din Cluj-Napoca
Samah Boudour
Algerian Research Center in Industrial Technologies: Centre de Recherche en Technologies Industrielles
Idris Bouchama
University of M'sila: Universite de M'sila
Bandar Astinchap (astinchap@gmail.com)
University of Kurdistan https://orcid.org/0000-0001-5401-3219
Hamta Ghanbaripour
Razi University of Kermanshah: Razi University

Research Article

Keywords: AFM, Mg doping, SEM, multifractal analysis, surface microtexture, ZnO thin films, XRD.

Posted Date: March 23rd, 2021

DOI: https://doi.org/10.21203/rs.3.rs-320908/v1

Multifractal analysis of ZnO thin films doped with Mg deposited by sol-gel spin coating on a glass substrate

Ştefan Ţălu [1,] , Samah Boudour [2], Idris Bouchama [3,4], Bandar Astinchap [5,6*], Hamta Ghanbaripour [7]

[1] Technical University of Cluj-Napoca, The Directorate of Research, Development and Innovation Management (DMCDI), 15 Constantin Daicoviciu St., Cluj-Napoca, 400020, Cluj county, Romania.

[2] Research Center in Industrial Technologies CRTI, P.O. Box 64, Cheraga, 16014, Algiers, Algeria.

[3] University of Msila, Faculty of Technology, Electronic Department, 28000, Msila, Algeria.

[4] University Ferhat Abbas, Research Unit on Emerging Materials (RUEM), Setif1, 19000, Algeria.

[5] University of Kurdistan, Faculty of Science, Department of Physics, 66177-15175, Sanandaj, Kurdistan, Iran.

[6] University of Kurdistan, Research Center for Nanotechnology, 66177-15175, Sanandaj, Kurdistan, Iran.

[7] Razi University, Faculty of Science, Physics Department, Kermanshah, Iran.

Corresponding author:

Prof. PhD. Bandar Astinchap

University of Kurdistan, Faculty of Science, Department of Physics, 66177-15175, Sanandaj, Kurdistan, Iran. E-mail: astinchap@yahoo.com

Conflict of interest: The authors do not have any possible conflict of interest.

ABSTRACT

A multifractal analysis has been performed on the three-dimensional surface microtexture of the ZnO thin films doped with Mg deposited by sol-gel spin coating on glass substrates. The effects of Mg doping element with amounts of 0, 2, 4, and 5 % on structural and morphological properties of the coated films were investigated. From the X-ray diffraction pattern analysis, it was found that the obtained thin films had a polycrystalline hexagonal wurtzite structure with preferential c-axis orientation and increased grain size with increasing the Mg doping. From scanning electron microscopy (SEM) analysis, it can be concluded that the surface of coated thin films had dense and uniformly distributed grains of nanoscale without any cracks over all surfaces of coated firms. From atomic force microscope (AFM) analysis, it can be also concluded that the surface of coated thin films had a dense columnar grain growth uniformly distributed over the entire 1 μm × 1 μm - scanned area. The surface microtexture was characterized in terms of multifractal analysis.

Keywords: AFM, Mg doping, SEM, multifractal analysis, surface microtexture, ZnO thin films, XRD.

1. INTRODUCTION

Diversity of structures and the excellent physical properties of metal oxide (MO) semiconductors offer a wide range of favorable features to be used in plethora of optoelectronic devices [1-5].

The monitoring of metal oxide experimental conditions like the deposition technique type, reagent, substrate, temperature, etc. has an important influence on the structure and properties of the semiconductor thin films [6]. On the other hand, the tuning or degeneration of the metal oxide systems by impurity doping, meaning, by a small addition of one or further metallic elements to form a thin film with further functional elements, is currently a scope of prime scientific concern. Among the potential metal oxides, zinc oxide (ZnO) thin films in their pure, doped [7-8] and co-

doped [9] forms have been processed widely by use of various techniques, especially the solution-based process, where, the overall process of obtaining microstructures ZnO thin films with high oriented crystallinity using the sol-gel techniques was very cost-effective and nontoxic.

Numerous researcher articles have recently focused on the preparation of ZnO thin films by sol-gel spin coating method [8, 10-11] because the spin coating is a simple oxide thin-film deposition technique, but it requires soluble types of reagents. Therefore, it is possible to control the ZnO film structures and their properties by the doping route. As an option, not an example, Mg^{2+} doping, which has an ionic radius of (0.57 Å) slightly smaller than the ionic radius of Zn^{2+} (0.60 Å) has been studied extensively [8-12], where, the incorporation of Mg elements in ZnO system tends to lighten the weight and to increases flexibility in the spinning process [8, 12].

Over the last decades, various studies were performed about the 3-D (three-dimensional) surface microtexture of thin films that allow extracting different topographic characteristics quantitatively for new technological applications [13-15]. On the other hand, the microtexture of the 3-D surface can be characterized by stereometric [16-18], fractal [19-21], and multifractal [22-25] analyzes with a set of parameters that highlight the particular morphological characteristics of the surface. Atomic force microscopy (AFM), in combination with modern image processing techniques, offers advanced facilities for extracting particular topographic features of surfaces and highlights the local nanoscale configuration of 3-D complex surfaces [26-28].

The objective of this study is to determine the 3-D surface microtexture of the spin-coated pure and magnesium doped ZnO thin films on glass substrates using AFM and multifractal analysis.

2. MATERIALS AND METHODS

2.1. Preparation of the samples

In this study, pure and zinc oxide films doped with Mg were ready by sol-gel spin coating method on glass substrates. Gel sols were prepared from the zinc acetate dihydrate [ZAD: ($Zn(CH_3COO)_2{\cdot}2H_2O$)] as the precursor, the Monoethanolamine [MEA: $H_2NCH_2CH_2OH$] as a stabilizer, the Isopropanol [2-Propanol: $CH_3CH(OH)CH_3$] as a solvent and the Magnesium chloride hexahydrate [$MgCl_2{\cdot}6H_2O$] as a source of Mg doping elements.

A 0.5 mol/l ZnO gel sols were prepared by dissolving 1.0974, 1.07550, 1.0535, 1.0425 mg of zinc acetate within an appropriate quantity of isopropanol (~10 ml) solvent. Then by adding different amounts of magnesium acetate (doping element), four ZnO sols were prepared. The Mg^{+2} doping elements were defined by Mg/(Mg+Zn) ratio, where they took the amount 0, 2, 4, and 5 %. A magnetic stirrer on a hot plate rigorously stirred the sols at a fixed temperature of 50°C for 15 minutes. By maintaining the molar ratio of MEA to zinc acetate at 1:1, the MEA was added drop-by-drop to the four alcoholic sols, where these sols were continuously heated accompanied by a magnetic stirrer for 2 hours at the same temperature (50 °C) to until a clear, colorless, homogenous sols were obtained. The yielded four gel sols were kept for 24 hours at room temperature. Using spin coater at a speed of 3000 rpm for 30 seconds, the four gel sols were spun onto four glass substrates that were pre-cleaned in an ultrasonic washer. The as-coated films were pre-heated at 250 °C for 4 minutes immediately after coating. After repeating the coating followed by a pre-heating procedure ten times, the films were annealed in a tube furnace at 500 °C for 90 minutes in the air.

2.2. Characterization techniques

The coated samples were characterized using X-ray diffractometer (XRD, BRUKER D8DISCOVER x-ray diffractometer, having a Cu Kα x-ray source) to check the structural properties and phase purity. The surface morphology and microstructure of each coated samples were characterized via scanning electron microscopy (SEM, ZEISS Gemini SEM 300).

The topography of the 3-D surface of the samples was analyzed by an atomic force microscope device (AFM, Bruker Dimension Icon AFM device operating in tapping mode), where all 512 × 512 pixels images were obtained by scanning square region of 1 μm × 1 μm.

2.3. The multifractal analysis of the thin film 3-D surface microtexture

The multifractal technique was applied to the AFM images by MATLAB software.

In literature, there are various methods to investigate the multifractality of the surface, and one of the most common is the box-counting method [13]. Therefore, we analyzed the AFM images of ZnO thin films using the box-counting method to study the multifractality of the effect of Mg doping, where it is briefly expressed below.

The AFM images are partitioned into the number of boxes to cover the images; therefore, P_{ij} is defined as following [13]:

$$P_{ij} = \frac{h_{ij}(\varepsilon)}{\left(\sum [h_{ij}(\varepsilon)]\right)} \quad (1)$$

P_{ij} is deposition probability (height distribution probability) in the box (i,j) and h_{ij} defines for the box (i,j) with ε size as average height. In terms of the Lipschitz-Holder exponent (α) we have [13]:

$$P_{ij}(\varepsilon) \sim \varepsilon^{\alpha} \quad (2)$$

$$N_{\alpha}(\varepsilon) \sim \varepsilon^{-f(\alpha)} \quad (3)$$

$N_{\alpha}(\varepsilon)$ is the number of boxes and $f(\alpha)$ is the singularity spectrum of α sub-datasets, which is known as a multifractal spectrum. In random multifractal, the singularity spectrum $f(\alpha)$ can be obtained using partition function $\chi_q(\varepsilon)$, as follow [13]:

$$\chi_q(\varepsilon) = \sum_{i,j} P_{ij}(\varepsilon)^q = \varepsilon^{\tau(q)} \quad (4)$$

where q ($-\infty < q < +\infty$) is called moment order.

$\tau(q)$ indicates mass exponent of order q [13]:

$$\tau(q) = lim_{\varepsilon \to 0} \frac{ln\chi_q(\varepsilon)}{\ln \varepsilon} \quad (5)$$

The exponent α and fractal dimension $f(\alpha)$ are obtained through Legendre transformation by the following equations [13]:

$$\alpha(q) = (d\tau(q))/dq \quad (6)$$

$$f(\alpha) = q\alpha(q) - \tau(q) \quad (7)$$

The value of q (moment order) in practice calculation is a finite number. The width of the multifractal spectrum is given by the relation $\Delta\alpha = \alpha_{max} - \alpha_{min}$ [13], which specifies the value of the $f(\alpha)$ in these values to obtain $\Delta f(\alpha)$. Some important parameters that can be obtained from the multifractal spectrum are $\Delta\alpha$, $\Delta f(\alpha)$, D_0 (capacity dimension), and D_1 (information dimension) [13].

2.4. Statistical analysis

All statistical analyses were performed using the software OriginPro 2016 (OriginLab, MA, USA). Variance analysis (ANOVA) was realized to compare the average values of the measures, and the pairs compared with Tukey post-hoc test, with significance levels of 5% ($p < 0.05$).

3. RESULTS

3.1. XRD analysis

The x-ray diffraction patterns as shown (Fig. 1) are used to examine the crystallographic structures of coated thin films and their phase purity. All the observed diffraction peaks (100), (002), (101), and (110) are related to the polycrystalline hexagonal wurtzite structure (Zincite, JCPDS 36-1451). Also, no impurity peaks, corresponding to MgO or Mg elements were detected in XRD patterns of coated films. To provide quantitative information of preferred orientation of crystallinity, the texture coefficient (TC_{hkl}) is calculated by the formula (8) and their calculated values are listed in Table 1:

$$TC_{hkl} = \frac{I(hkl)/I_0(hkl)}{\frac{1}{n}\sum_1^n I(hkl)/I_0(hkl)} \quad (8)$$

where $I(hkl)$ is the measured intensity of the diffraction (hkl) peak, $I_0(hkl)$ is the standard intensity given in the reference JCPDS pattern that matches with the taken (hkl) peak from the analyzed XRD patterns, and n is the number of diffraction peaks considered.

The Scherrer equation has been used to calculate the average microcrystalline size (grain size) of the polycrystalline thin films and its formula (9) [11] is:

$$D = \frac{0.9\,\lambda}{\beta\,cos(\theta)}\ (nm) \quad (9)$$

where λ, θ, and β are the wavelength of X-ray CuKα (λ = 1,54056 Å), Bragg diffraction angle, Full width at half maximum (FWHM) of XRD peaks, respectively.

By using Bragg's law and the hexagonal system equation, the cell parameters c-length and a-length axes and their ratio c/a are calculated by tacking the (100) and (002) XRD peaks as expressed by the following formula (10) [11]:

$$a = \frac{\lambda}{\sqrt{3}sin(\theta_{100})} \quad (10a)$$

$$c = \frac{\lambda}{sin(\theta_{002})} \quad (10b)$$

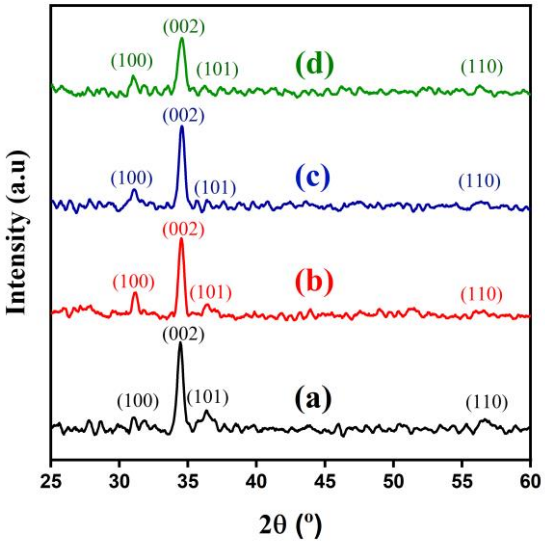

Fig. 1. XRD diffraction patterns of deposited ZnO thin films with different percentage of Mg doping: a) pure ZnO; b) ZnO doped with %2 Mg; c) ZnO doped with %4 Mg; d) ZnO doped with %5 Mg.

Table 1. Calculated parameters from XRD spectrum of layers in Fig. 1.

The XRD parameters		ZnO thin films with different Mg doping			
		Pure ZnO	Doped with %2	Doped with %4	Doped with %5
2θ (degree) of (002) peak		34.5123	34.5135	34.5251	34.5889
TC	(100)	0.34	0.14	0.24	0.34
	(002)	2.92	2.51	3.14	2.54
	(101)	0.49	0.38	0.21	0.28
FWHM		0.243257	0.219342	0.142039	0.167813
D [nm]		34.20	37.92	58.57	49.58
Cell parameter	a [nm]	3.243	3.247	3.260	3.241
	c [nm]	5.193	5.193	5.191	5.182
	c/a	1.601	1.599	1.592	1.598

It is clear, as shown in fig. 1 that the four samples have prominent and narrowest peaks at the plane (002). Furthermore, as recorded in Table 1, these prominent and narrowest (002) peaks are located around (2θ ~ 34.5°) and showed TC values higher than that of the other recorded main peaks. These observations indicate that the phase reflection of the preferential orientation of micro-crystallinity is following (002) plane along the *c*-axis.

The grain size of coated samples, as listed in Table 1 had an opposite tendency compared to the full width at half maximum (FWHM) of (002) peak. Where, the coated ZnO thin films doped with 0, 2 and 4 % have increased grain sizes of 34.20, 37.92, and 58.57 nm, respectively. While the grain size tends to decrease again at film doped with 5 % of Mg to 49.58 nm. In general, this increasing trend means that high Mg incorporation within ZnO films causes grain size to increase.

Siregar et al. [12] found that the increase in Mg concentration within ZnO lattice increases the grain size and causes a gradation in crystal quality, crystal defects, and crystal distortion. In addition to the decrease of its FWHM-broadening, the (002) peak slightly shifted to higher angles compared to that of pure ZnO film as determined in Table 1. As per the Braggs law, such tendency can be explained by the substitution of Zn^{2+} by Mg^{2+}, which has an atomic radius slightly smaller than that of the Zn^{2+}. Where, this slight difference causes the slight shirking in the lattice plane hence a crystalline defectiveness will be induced that leads to shifting of major (002) peak to higher angle [9]. As shown in Table 1, the cell parameters *c*-length was decreased drastically from 5.193 nm for pure ZnO film to 5.182 nm for the ZnO film doped with 5 % of Mg compared to the wavering decrease of *a*-length. The listed ratio *c/a* in Table 1 sums the changes of *a*- and *c*-axes to express the change rate in the structure. Where, the ZnO film doped with 4 % of Mg showed the low ratio, which means that the change in the two directions *a*- and *c*-axes was the most comparable and lead to the high grain size. At this change rate, the grain size was as high as 58.57 nm. Such high grain size may attribute to the smaller grains that have sufficient driving force to undergo diffusion to form bigger grains [12].

3.2. SEM analysis

Fig. 2 shows the surface morphology of spin-coated and annealed ZnO thin films doped with Mg that were assessed by scanning electron microscopy (SEM). These SEM images reveal that the grain sizes depend on the amount of Mg concentration within the film. All films showed extremely dense and uniformly distributed nano-sized grains overall surface area with even no cracks or voids. Also, the ZnO thin film doped by 4 % of Mg showed a higher grain size.

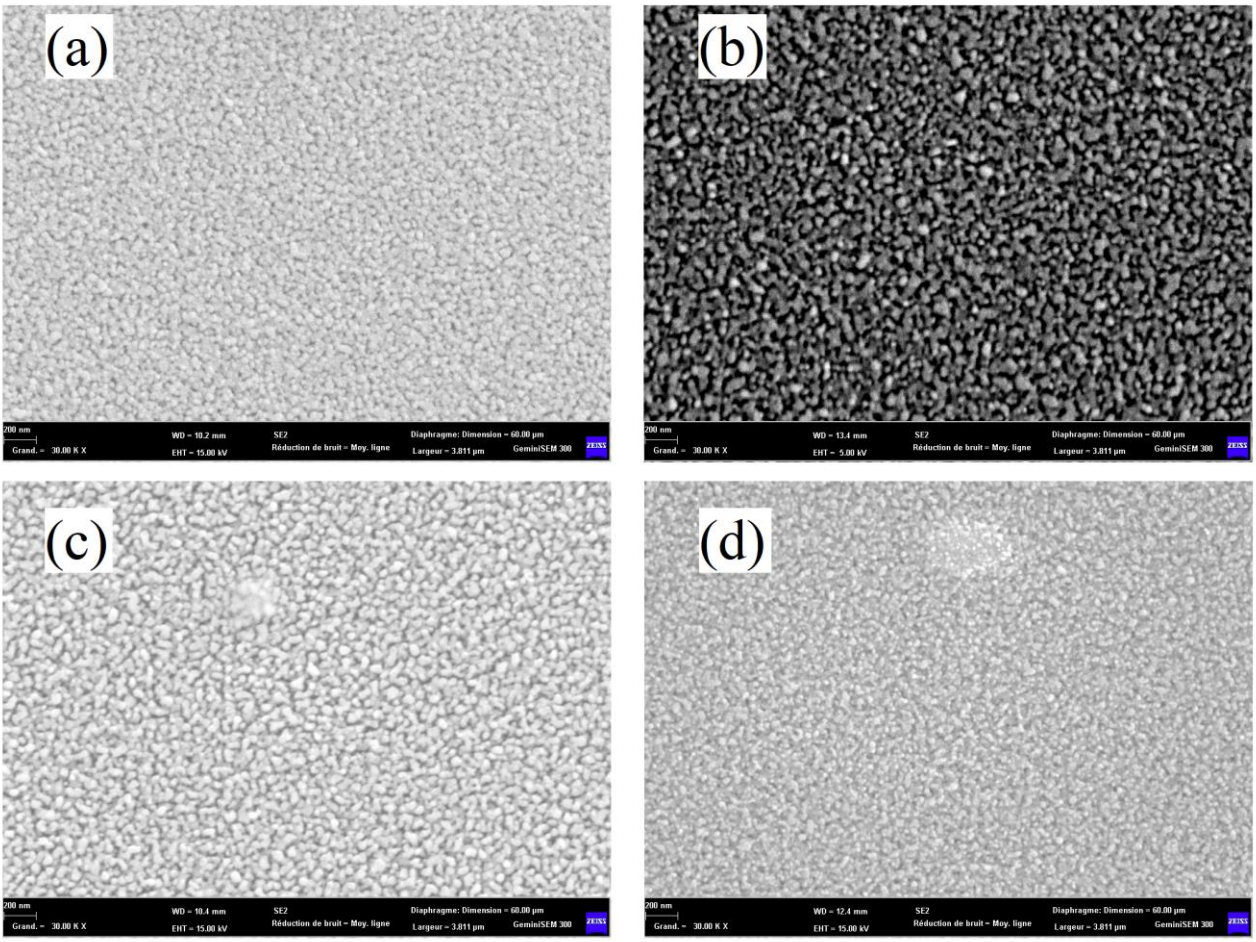

Fig. 2. SEM images of deposited ZnO thin films with different percentage of Mg doping: a) pure ZnO; b) ZnO doped with %2 Mg; c) ZnO doped with %4 Mg; d) ZnO doped with %5 Mg.

3.3. AFM measurements

The representative 3-D AFM images are shown in fig. 3. These images show the growth of dense columnar granules uniformly distributed on the entire scanned surface. These grains are interspersed by small and deep pits. Also, the spikes of these grains are sharp for the pure film fig. 3(a). When Mg doping is increased, the spikes tend to flatten out, as shown in fig. 3(b, c, and d). To find out how is the change in surface morphology of ZnO thin films with Mg doping, the AFM images (fig. 3) of the layers were analyzed using a multifractal technique.

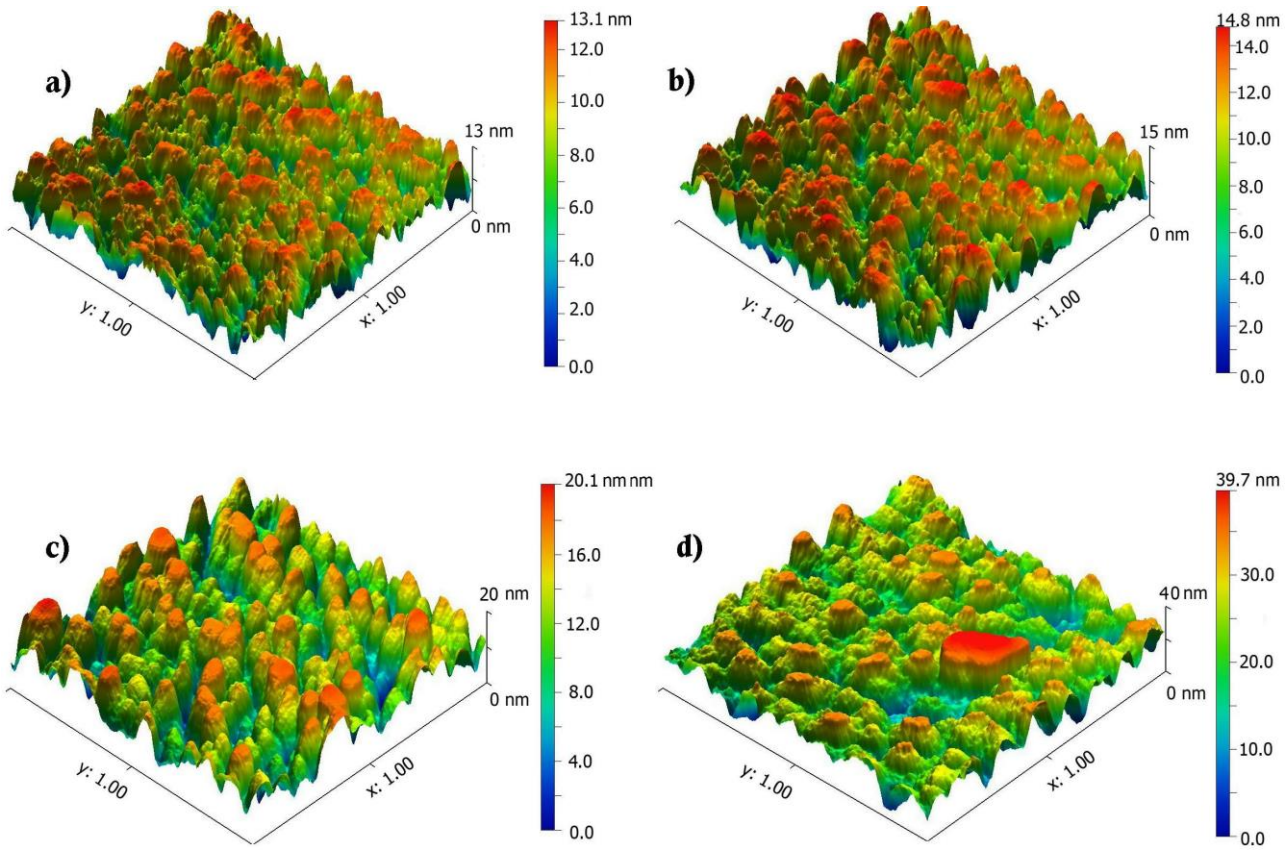

Fig. 3. AFM images of deposited ZnO thin films with different percentage of Mg doping: a) pure ZnO; b) ZnO doped with %2 Mg; c) ZnO doped with %4 Mg; d) ZnO doped with %5 Mg.

The $ln\chi_q(\varepsilon)$ curves vs. $ln\varepsilon$ for the ZnO thin films with different doping of Mg is plotted in fig. 4. The figure shows that the curves are linear for all four thin films.

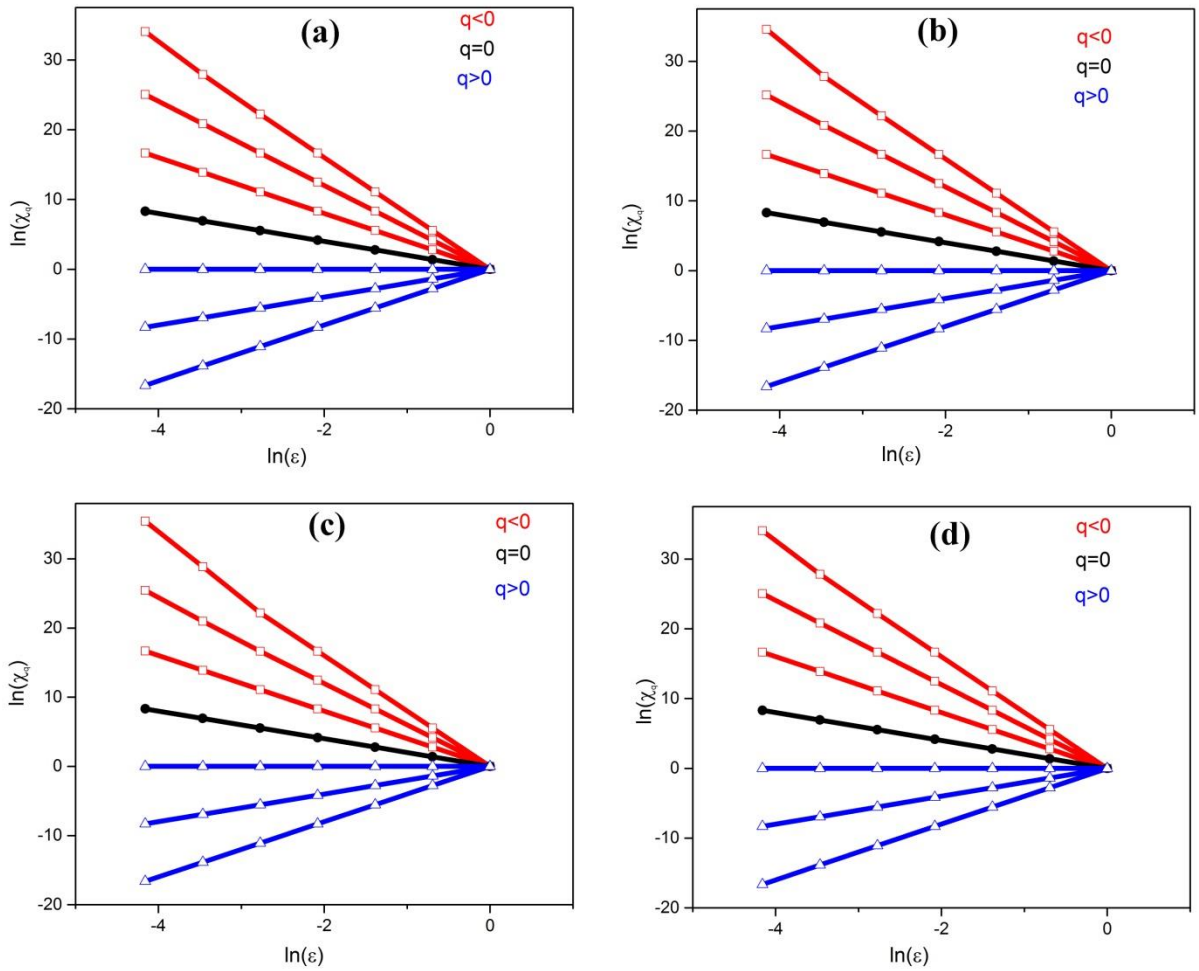

Fig. 4. $\ln\chi_q(\varepsilon)$ versus $\ln\varepsilon$ for the ZnO thin films with different percentage of Mg doping: (a) pure ZnO, (b) ZnO doped with %2 Mg, (c) ZnO doped with %4 Mg, (d) ZnO doped with %5 Mg.

By using eq (5), the *τ(q)* was obtained as a function of q for all samples, which is shown in fig. 5. The results show that the curve of *τ(q)* has a nonlinear response for all samples. Nonlinear and linear mass exponent and partition function curves, respectively, indicate that surfaces of the deposited ZnO thin films are multifractal.

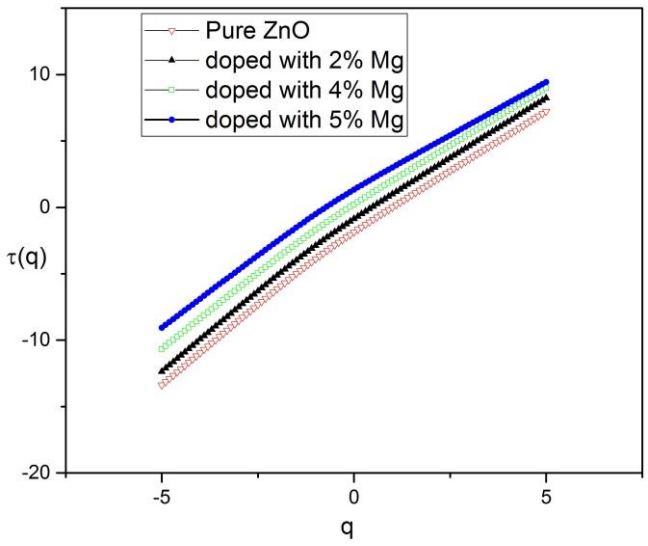

Fig. 5. τ(q) as a function of q for the ZnO thin films with different percentage of Mg doping.

The multifractal spectrum obtained from the multifractal analysis of these images using the Matlab software is shown in Fig. 6. The data obtained from the multifractal spectrum including α_{min}, α_{max}, $\Delta\alpha$, $f(\alpha_{min})$, $f(\alpha_{max})$, $\Delta f(\alpha)$, $\alpha(q=0)$ and $f_{max}(\alpha) = f(q=0) = D_0$ (capacity dimension) are listed in the table 2.

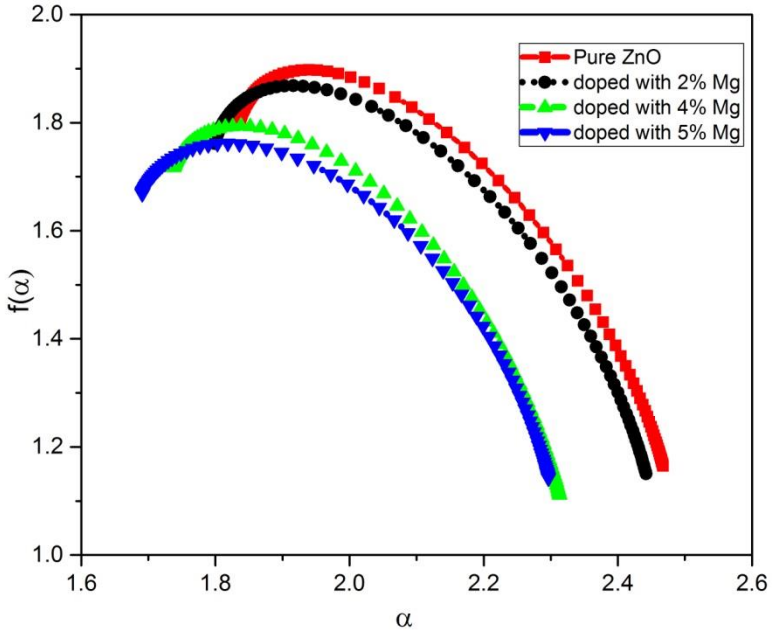

Fig. 6. The curve of the f(α) in terms of α, as a multifractal spectrum, for the ZnO thin films with different percentage of Mg doping.

The data obtained show that Mg doping in ZnO thin films and increasing its percentage to 4% decreases $\Delta\alpha$ and then with increasing doping to 5% the $\Delta\alpha$ increases. It means that the multifractal spectrum for the ZnO thin film with Mg doping becomes narrower up to a percentage of 4%. This indicates that the complexity and multifractality of the ZnO surface is decreased, but with more increasing Mg doping, it increases.

The obtained data in table 2 show that the sign of Δf is positive and its value decreases with increasing doping Mg in ZnO thin films. The sign of the Δf is attributed to how deposition distributes at the highest and lowest sites on the surface of layers. Therefore, when the sign of Δf is positive, it means that the deposition tends to be lying at the highest sites than the lowest sites on the surface of layers. These results show that large-scale events determine the surface behavior and are the dominant phenomenon on the surface of the ZnO thin films. Also, it can be concluded that the growth of the ZnO thin films has followed Volmer-Weber (island formation) mechanism and this growth mechanism of ZnO layers becomes more dominant with the Mg doping.

Table 2. Obtained parameters from multifractal spectrum of layers in fig. 6.

The multifractal parameters	ZnO thin films with different Mg doping			
	Pure ZnO	Doped with %2	Doped with %4	Doped with %5
D_0	1.8976	1.8684	1.7938	1.7918
D_1	1.8178	1.7893	1.7387	1.6800
A_0	1.9392	1.9162	1.8380	1.8186
A_1	1.8399	1.8054	1.7414	1.6950
α_{max}	2.4974	2.4419	2.3131	2.2966
α_{min}	1.8346	1.7990	1.7377	1.6909

$\Delta\alpha = \alpha_{max} - \alpha_{min}$	0.6628	0.6429	0.5754	0.6057
f_0	1.8976	1.8684	1.7938	1.7918
f_1	1.8178	1.7893	1.7387	1.6800
$f(\alpha_{min})$	1.7974	1.7613	1.7172	1.6687
$f(\alpha_{max})$	1.1664	1.1506	1.1110	1.1420
$\Delta f = f(\alpha_{min}) - f(\alpha_{max})$	0.6328	0.6107	0.6062	0.5267

4. CONCLUSIONS

Pure and ZnO thin films doped with Mg were deposited on glass substrates using the sol-gel spin coating method. Different amounts of Mg (0, 2, 4, and 5 %) doping elements were used to modify the structure in a nanometer scale. After investigating the coated films by XRD, SEM, and AFM devices, it turns out that the Mg doping has stark effects on the structural and morphological properties of these ZnO thin films. As a result, XRD analysis revealed that the pure and ZnO thin films doped with Mg had wurtzite crystalline structures with nanoscale grains of size hovering in the range of 34.20 - 58.57 nm. Besides, the presence of these grains was dense and distributed uniformly over all the surfaces, as shown by the SEM analysis. Furthermore, AFM analysis revealed that the grains had columnar growth and were interspersed by small and deep pits on the entire scanned surface. But, from AFM micrographs the coated ZnO thin films doped with Mg on glass substrate exhibit the appropriate surface quality, which is hold promising for use as an absorber in thin films solar cells, as an electrode in biosensors also in other modern technological applications.

ORCID

Ştefan Ţălu, http://orcid.org/0000-0003-1311-7657.

Bandar Astinchap, https://orcid.org/0000-0001-5401-3219.

Samah Boudour, https://orcid.org/0000-0002-4277-6945.

Credit author statement

Ştefan Ţălu: conceptualization, methodology. Samah Boudour: investigation, data curation, original draft preparation. Idris Bouchama: supervision, reviewing. Bandar Astinchap: multifractal analyses, validation. Hamta Ghanbaripour: multifractal analyses, visualization. All authors have read and agreed to the published version of the manuscript.

The data availability statement: The data that support the findings of this study are available from the corresponding author upon reasonable request.

ACKNOWLEDGMENTS

The authors would like to thank to Assist. Prof. Dr. Eng. Faouzi Ghribi from the National Engineering School of Gabes - University of Gabès (LaPhymne), Avenue Omar Ibn El Khattab, Zrig Gabes, 6029, Tunisia, for his useful comments.

5. REFERENCES

[1] Z. Cao, C. Li, X. Deng, S. Wang, Y. Yuan, Y. Chen, Z. Wang, Y. Liu, L. Ding, F. Hao, , J. Mater. Chem. A, 8, 19768 (2020). DOI: 10.1039/d0ta07282f.

[2] S. Laidoudi, M.R. Khelladi, L. Lamiri, S. Boudour, C. Dehchar, R. Boufnik,. Appl. Phys. A, 127, 160 (2021). DOI: 10.1007/s00339-021-04299-x.

[3] D. Dimitrov, C.-L. Tsai, S. Petrov, V. Marinova, D. Petrova, B. Napoleonov, B. Blagoev, V. Strijkova, k.Y. Hsu, S.H. Lin, Coatings, 10, 539 (2020). DOI: 10.3390/coatings10060539.

[4] S. Boudour, I. Bouchama, M. Hadjab, S. Laidoudi, Opt. Mater., 98, 109433 (2019). DOI: 10.1016/j.optmat.2019.109433.

[5] P. Meng, C. Yuan, H. Xu, S. Wan, Q. Xie, J. He, H. Zhao, J. Hu, J. He, Electr. Power Syst. Res., 178, 106041 (2020). DOI: 10.1016/j.epsr.2019.106041.

[6] Ü. Özgür, Ya. I. Alivov, C. Liu, A. Teke, M.A. Reshchikov, S. Doğan, V. Avrutin, S.-J. Cho, H. Morkoç, J Appl Phys., 98, 041301 (2005). DOI: 10.1063/1.1992666.

[7] O. Urper, N. Baydogan, Mater Lett., 274, 128000 (2020). Doi:10.1016/j.matlet.2020.128000.

[8] N. H. Hashim, S. Subramani, M. Devarajan, A. R. Ibrahim, J Aust Ceram Soc., 53, 421 (2017). DOI: 10.1007/s41779-017-0051-9.

[9] I. Y. Kim, S. W. Shin, M. G. Gang, S. H. Lee, K. V. Gurav, P. S. Patil, J. H. Yun, J. Y. Lee, J. H. Kim, Thin Solid Films, 570, 321 (2014). DOI:10.1016/j.tsf.2014.02.109.

[10] K. Verma, B. Chaudhary, V. Kumar, V. Sharma, M. Kumar, Vacuum, 146, 524 (2017). DOI: 10.1016/j.vacuum.2017.06.031.

[11] M.N.H. Mia, M.F. Pervez, M.K. Hossain, H.K. Ghosh, M. Hoq, M.R. Rahman, M. Jalal Uddin; M.A. Al Mashud, 7, 2683 (2017). DOI: 10.1016/j.rinp.2017.07.047.

[12] N. Siregar, Motlan, D. J. Panggabean, J. Phys.: Conf. Ser., 1428, 012026 (2020) . DOI: 10.1088/1742-6596/1428/1/012026.

[13] Ş. Ţălu, Napoca Star Publishing House, Cluj-Napoca, Romania, 2015.

[14] Ş. Ţălu, M. Bramowicz, S. Kulesza, S. Solaymani, A. Ghaderi, L. Dejam, A. Boochani, S. Mohammad Elahi, Superlattices Microstruct. 93, 109 (2016). DOI: 10.1016/j.spmi.2016.03.003.

[15] Ş. Ţălu, S. Stach, M. Ikram, D. Pathak, T. Wagner, J.M. Nunzi, Int. J. Nanosci., 13(3), 1450020 (2014). DOI: 10.1142/S0219581X14500203.

[16] A. Jafari, M.H. Alam, D. Dastan, S. Ziakhodadadian, Z. Shi, H. Garmestani, A.S. Weidenbach, Ş. Ţălu, J. Mater. Sci. Mater. Electron., 30(24), 21185 (2019). DOI: 10.1007/s10854-019-02492-6.

[17] Ş. Ţălu, M. Bramowicz, S. Kulesza, A. Ghaderi, V. Dalouji, S. Solaymani, Z. Khalaj, Mater. Lett., 12(5), 580 (2016). DOI: 10.1007/s13391-016-6036-y.

[18] A. Méndez, Y. Reyes, G. Trejo, K. Stępień, Ş. Ţălu, Microsc. Res. Tech., 78, 1082 (2015). DOI: 10.1002/jemt.22588.

[19] F.M. Mwema, E.T. Akinlabi, O.P. Oladijo, O.S. Fatoba, S.A. Akinlabi, Ş. Ţălu, K. Kumar, J.P. Davim (eds.) Modern Manufacturing Processes, 1st ed., section 1, chapter 2, pp. 13-39. DOI: 10.1016/B978-0-12-819496-6.00002-6. Woodhead Publishing Reviews: Mechanical Engineering Series, USA, 2020.

[20] Ş. Ţălu, A.J. Ghazai, S. Stach, H. Abu Hassan, Z. Hassan, M. Ţălu, J. Mater. Sci. Mater. Electron., 25(1) 466, (2014). DOI: 10.1007/s10854-013-1611-6.

[21] Ş. Ţălu, S. Stach, D. Raoufi, F. Hosseinpanahi, Electron. Mater. Lett., 11(5) 749, (2015). DOI: 10.1007/s13391-015-4280-1.

[22] Ş. Ţălu, S. Stach, A. Mahajan, D. Pathak, T. Wagner, A. Kumar, R.K. Bedi, M. Ţălu, Electron Mater Lett., 10(4), 719 (2014). DOI: 10.1007/s13391-013-3270-4.

[23] B. Astinchap, H. Ghanbaripour, R. Amuzgar, Optik, 222, 165384 (2020). DOI: 10.1016/j.ijleo.2020.165384.

[24] Ş. Ţălu, S. Stach, S. Valedbagi, R. Bavadi, S. M. Elahi, M. Ţălu, Mater Sci-Poland, 33(3), 541 (2015). DOI: 10.1515/msp-2015-0086.

[25] Ş. Ţălu, I.A. Morozov, R.P. Yadav, Appl Surf Sci., 484, 892 (2019). DOI: 10.1016/j.apsusc.2019.04.170.

[26] D. Sobola, Ş. Ţălu, S. Solaymani, L. Grmela, Microsc. Res. Tech., 80(12), 1328 (2017). DOI: 10.1002/jemt.22945.

[27] S. Stach, W. Sapota, Ş. Ţălu, A. Ahmadpourian, C. Luna, N. Ghobadi, A. Arman, M. Ganji, J. Mater. Sci. Mater. Electron., 28(2), 2113 (2017). DOI: 10.1007/s10854-016-5774-9.

[28] Ş. Ţălu, C. Luna, A. Ahmadpourian, A. Achour, A. Arman, S. Naderi, N. Ghobadi, S. Stach, B. Safibonab, J. Mater. Sci. Mater. Electron., 27(11), 11425 (2016). DOI: 10.1007/s10854-016-5268-9.

Figures

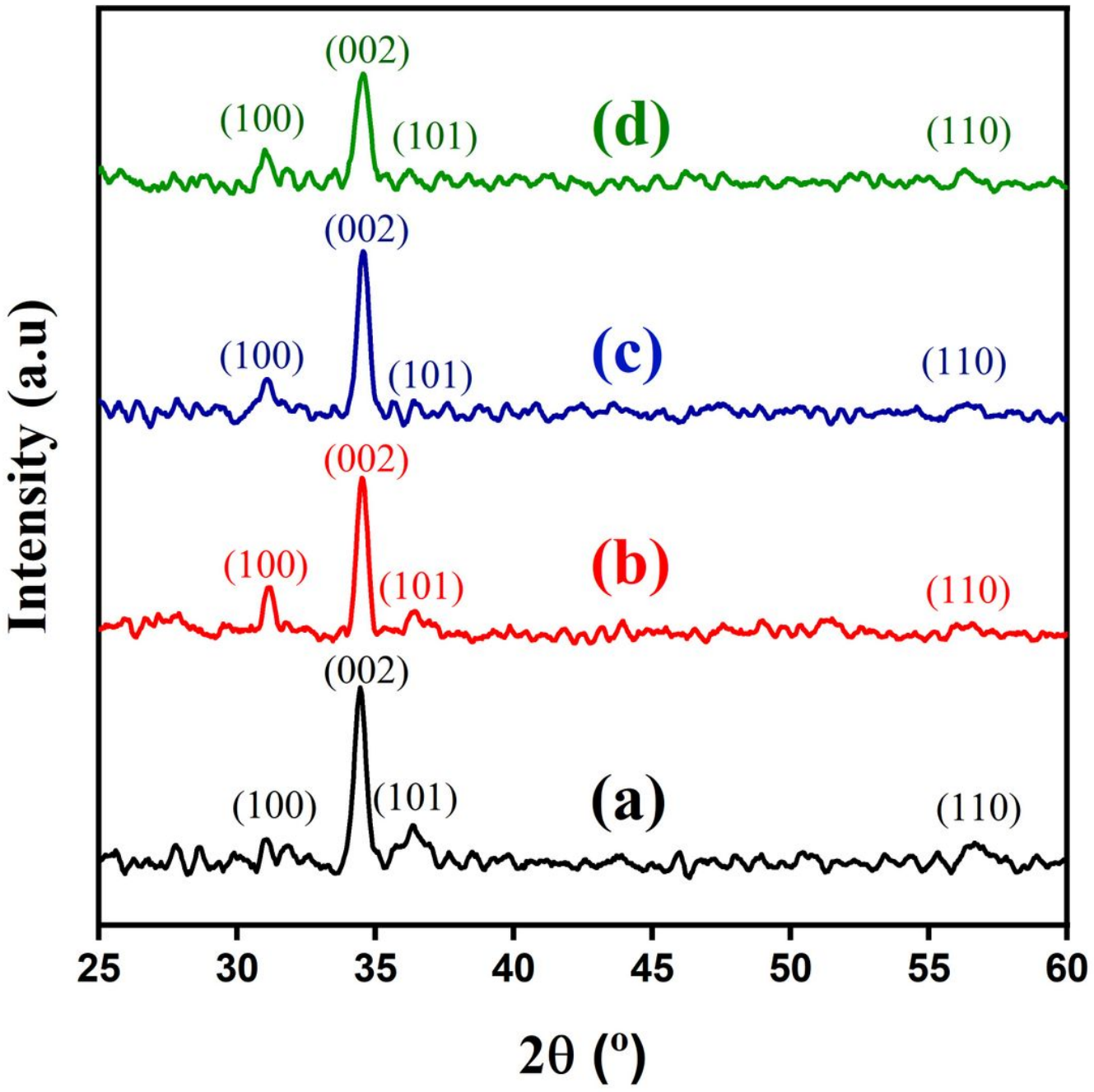

Figure 1

XRD diffraction patterns of deposited ZnO thin films with different percentage of Mg doping: a) pure ZnO; b) ZnO doped with %2 Mg; c) ZnO doped with %4 Mg; d) ZnO doped with %5 Mg.

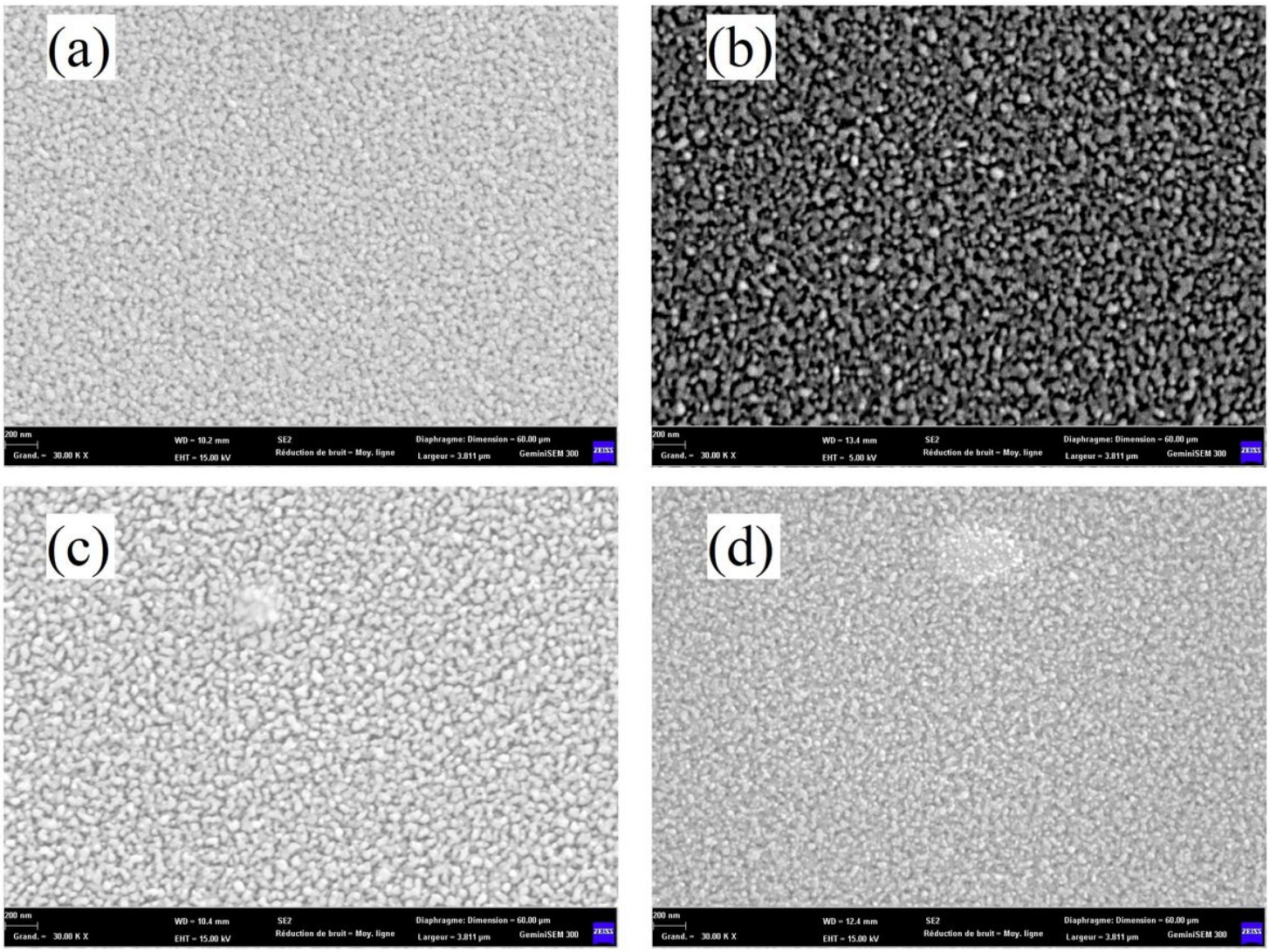

Figure 2

SEM images of deposited ZnO thin films with different percentage of Mg doping: a) pure ZnO; b) ZnO doped with %2 Mg; c) ZnO doped with %4 Mg; d) ZnO doped with %5 Mg.

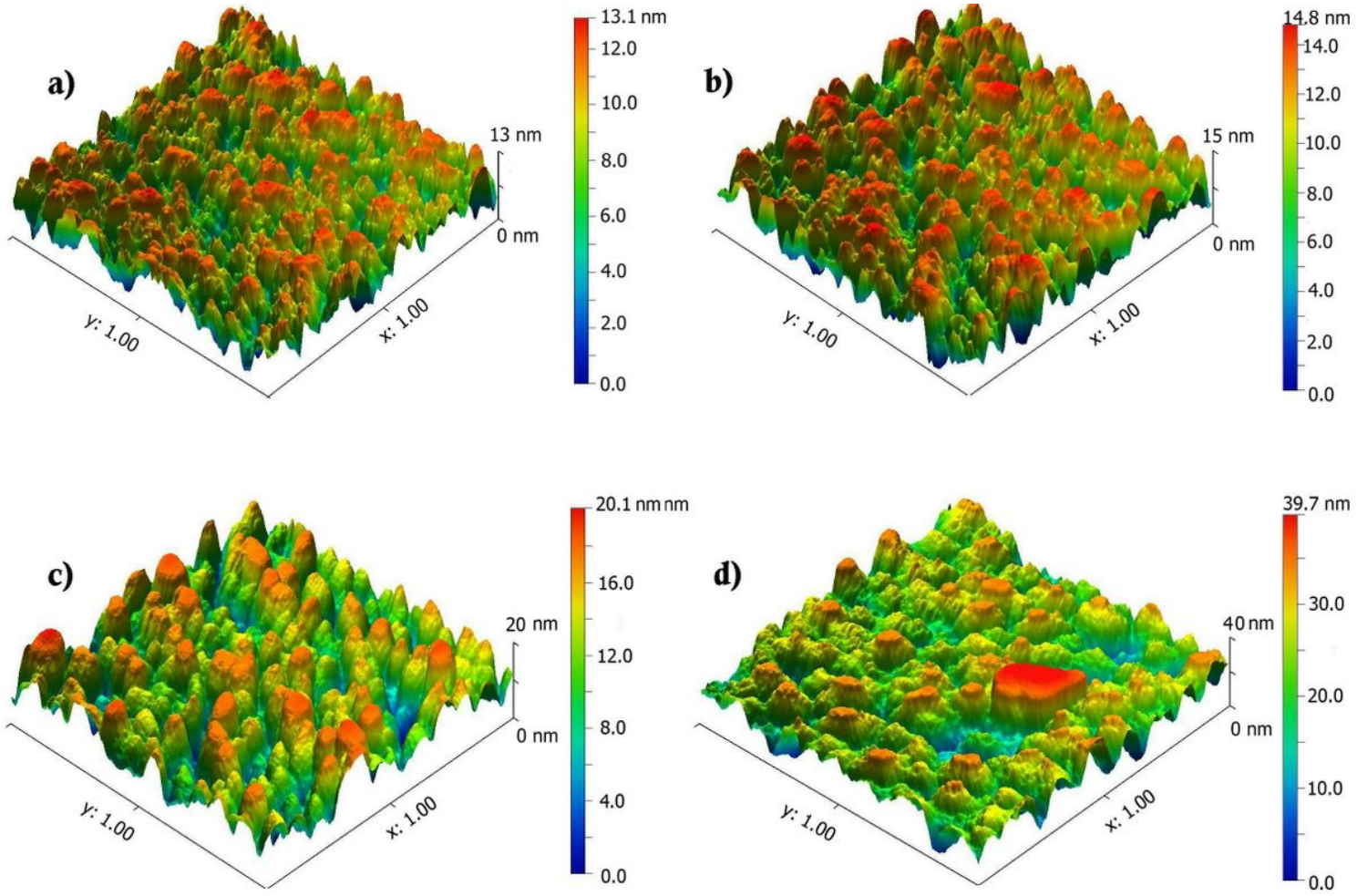

Figure 3

AFM images of deposited ZnO thin films with different percentage of Mg doping: a) pure ZnO; b) ZnO doped with %2 Mg; c) ZnO doped with %4 Mg; d) ZnO doped with %5 Mg.

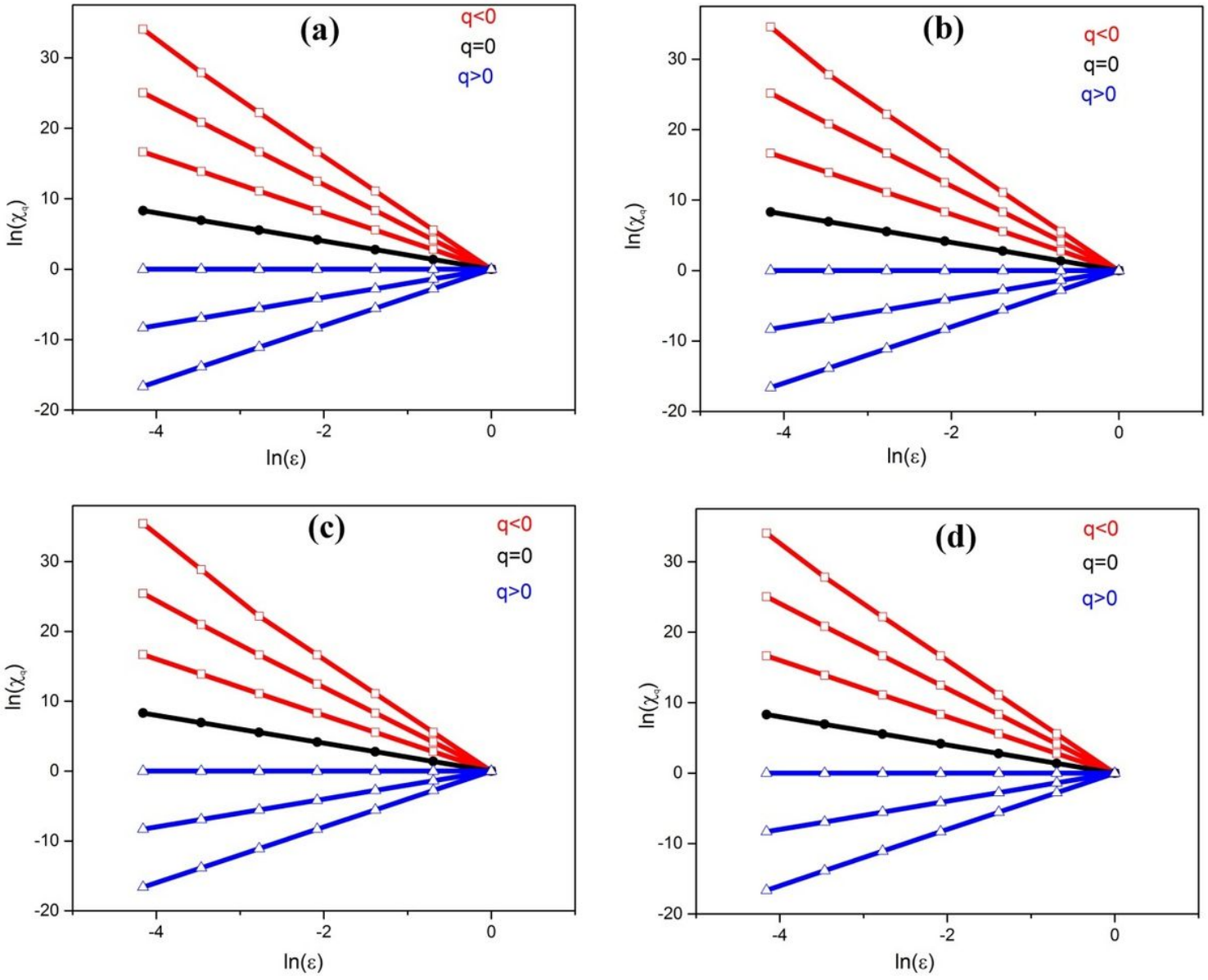

Figure 4

lnχq(ε) versus ln for the ZnO thin films with different percentage of Mg doping: (a) pure ZnO, (b) ZnO doped with %2 Mg, (c) ZnO doped with %4 Mg, (d) ZnO doped with %5 Mg.

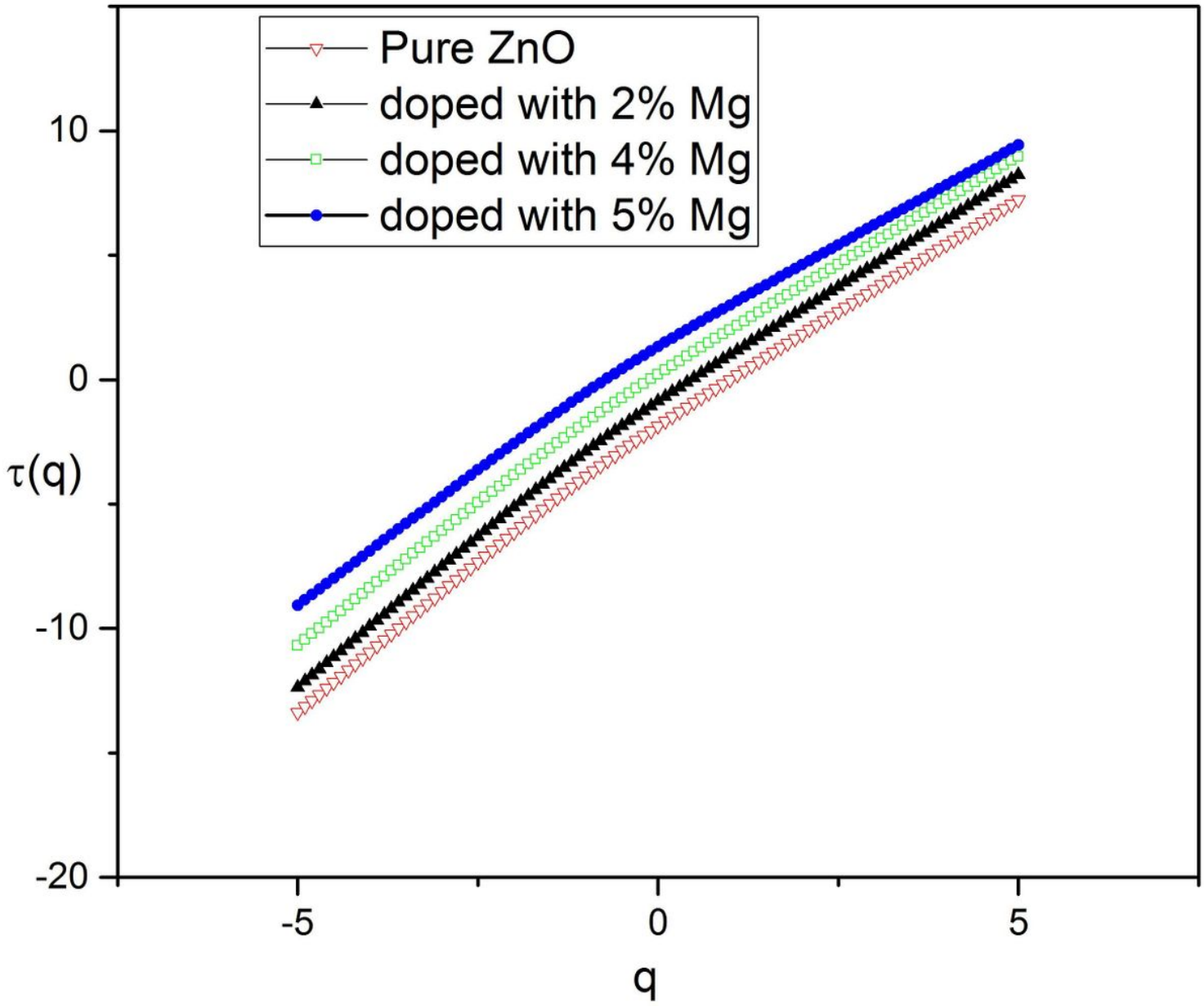

Figure 5

τ(q) as a function of q for the ZnO thin films with different percentage of Mg doping

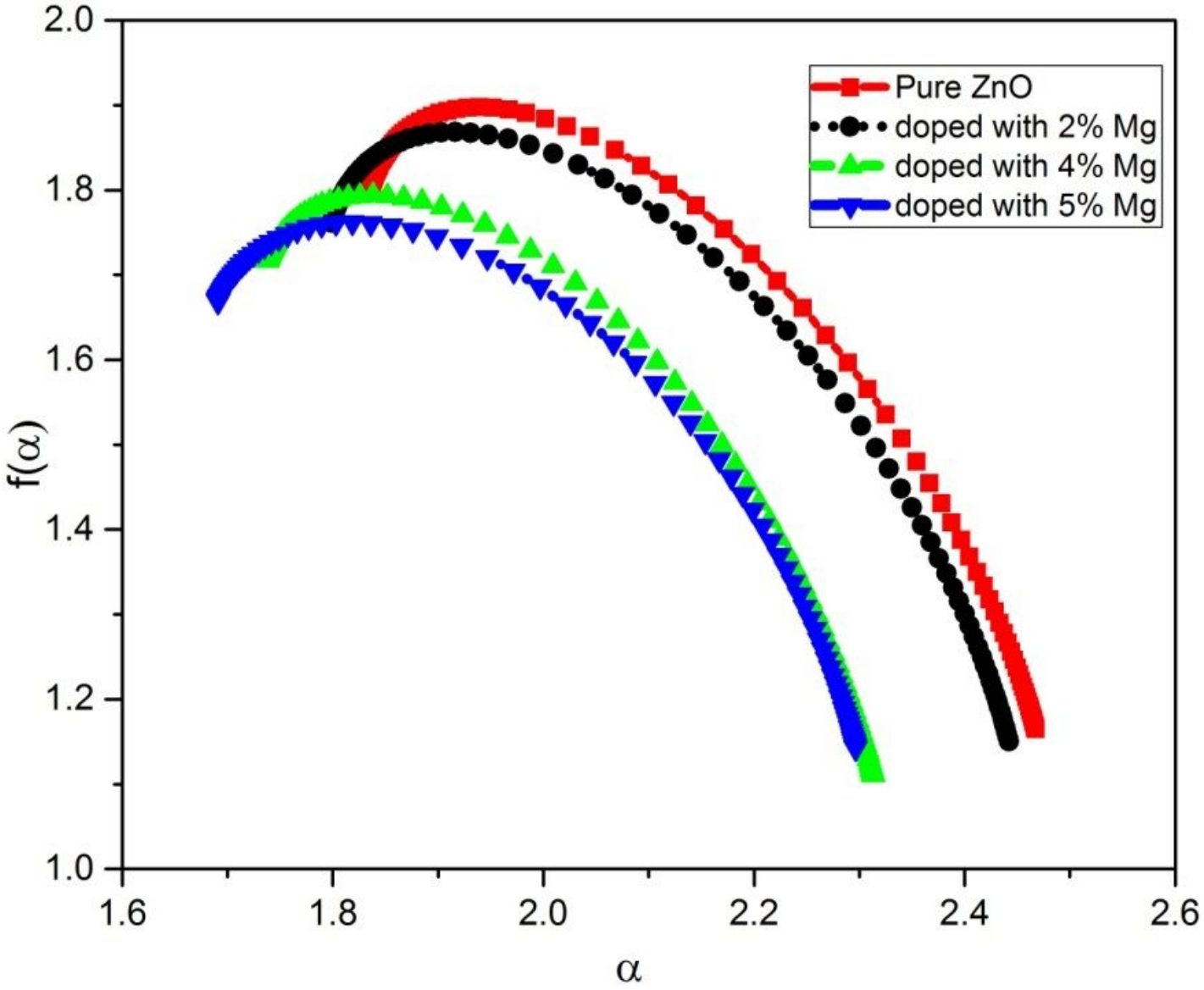

Figure 6

The curve of the f(α) in terms of α, as a multifractal spectrum, for the ZnO thin films with different percentage of Mg doping.